Supplementary information for:

Catenation and Encapsulation Induce Distinct Reconstitutions Within a Dynamic Library of Mixed-ligand Zn_4L_6 Cages

Samuel P. Black, Daniel M. Wood, Felix B. Schwarz, Tanya K. Ronson, Julian J. Holstein, Artur R. Stefankiewicz, Christoph A. Schalley, Jeremy. K. M. Sanders,* and Jonathan R. Nitschke**

Table of Contents

1 Experimental Methods

Unless otherwise specified all solvents and reagents were purchased from commercial sources and used as supplied. NMR spectra were recorded on Bruker DRX-400 MHz or Bruker Avance 500 Cryo spectrometers. ^{1}H chemical shifts (δ) are reported in parts per million (ppm) and are reported relative to the solvent residual resonances. Unless otherwise stated, all spectra were recorded at 298K.

Electrospray ionization Fourier-transform ion-cyclotron resonance (ESI-FTICR) MS(/MS) experiments were conducted with an Ionspec QFT-7 FTICR mass spectrometer (Agilent Technologies, Lake Forest, CA, USA), equipped with a 7 T superconducting magnet and a Micromass Z-spray ESI source (Waters Co., Saint-Quentin, France). The samples were introduced into the ion source at flow rates of 2 – 4 μL/min. A constant spray and highest intensities were achieved with a capillary voltage of 4400 V and a source temperature of 313 K. The parameters for sample cone (17 V) and extractor cone (8 V) voltages as well as the ion optics were optimized for maximum abundances of the desired complex ions. Multiple scans (up to 20) were averaged for each spectrum in order to improve the signal-to-noise ratio.

2 Synthesis of NDI diamine 1

1,4,5,8-naphthalenetetracarboxylic dianhydride (1.00 g, 3.73 mmol) and 1,4-diaminobenzene (1.00 g, 9.33 mmol) were suspended in 40 mL of dry DMF, in a 100 mL round bottom flask and sonicated for 30 min. Triethylamine (2.6 mL, 18.7 mmol) was added and the reaction mixture was heated to reflux for 10 min at 140 ± 5 °C under microwave irradiation. The resulting mixture was filtered and the residue was washed with copious amounts of water, acetone and then chloroform. NDI **1** was isolated as a dark brown powder (1.55 g, 93%) and was used without further purification. ^{1}H NMR (400 MHz: [D_6]-DMSO) δ = 8.70 (4H, s, H^4), 7.03 (4H, d, J = 8.5 Hz, H^3) 6.69 (4H, d, J = 8.5 Hz, H^2) 5.32 (4H, s, H^1). ^{13}C NMR (125 MHz: [D_6]-DMSO): δ = 164.2. 149.8, 131.4, 130.1, 127.9, 127.5, 124.2, 114.6. HRMS, (EI^+) calcd. for $C_{26}H_{16}N_4O_4[M^+]$ *m/z* : 448.1172, found: 448.1171

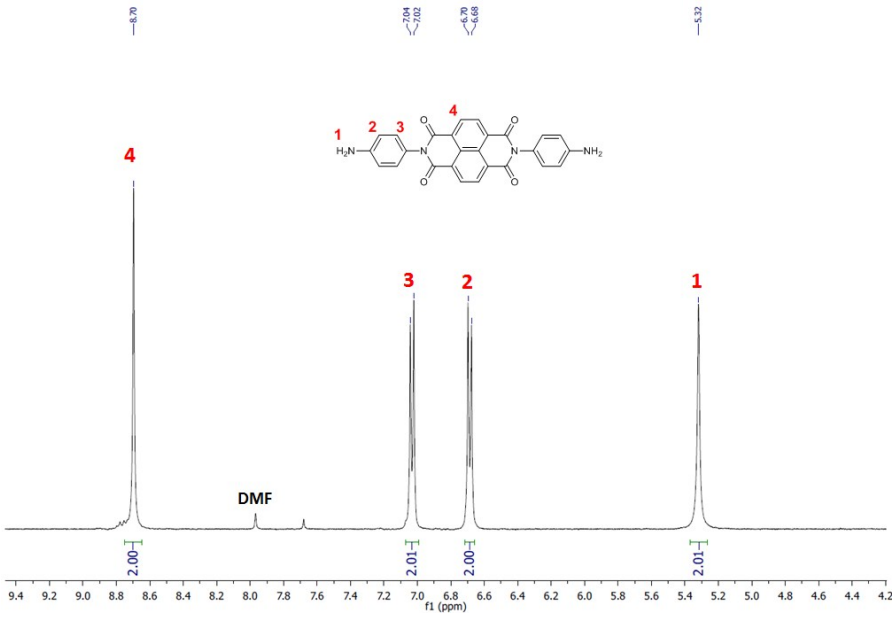

Figure S1. ^{13}C NMR (400 MHz: [D_6]-DMSO) of NDI ligand **1**.

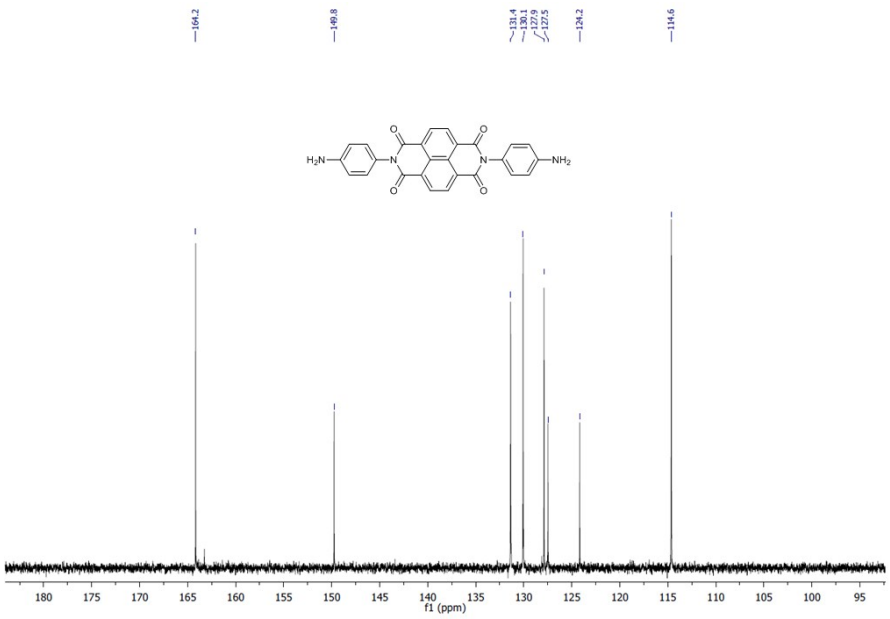

Figure S2. ^{13}C NMR (500 MHz: $[D_6]$-DMSO) of NDI ligand **1**.

3 Synthesis of cage N_6

NDI **1** (224 mg, 0.5 mmol), zinc(II) triflimide (208 mg, 0.33 mmol) and 2-formylpyridine (95 µL, 1.0 mmol) were combined in MeCN (20 mL). The flask was heated at 50 °C under N_2 for 24 h. The crude product was purified by filtration through Celite and precipitation with diethyl ether. The resultant dark yellow crystalline solid was isolated and washed with excess diethyl ether (349 mg, 67%). ^1H NMR (500 MHz: $CD_3CN/CHCl_3$ 1:1) δ = 8.75-8.61 (3H, m, H^5 & H^8), 8.50-8.48 (1H, m, H^3), 8.34-8.28 (1H, m, H^4), 8.25-8.07 (1H, m, H^1), 7.97-7.94 (1H, m, H^2), 7.43-7.32 (2H, m, H^7), 6.33-6.00 (2H, m, H^6).^{13}C NMR (125 MHz: $CD_3CN/CHCl_3$ 1:1) δ = 166.6, 166.0, 165.8, 164.4, 164.3, 151.0, 150.8, 149.0, 148.9, 148.7, 147.4, 144.3, 136.5, 136.2, 136.0, 132.4, 132.2, 131.9, 128.6, 128.4, 128.4, 128.3, 128.3, 124.9, 123.1, 122.4, 119.8, 117.2. *m/z* (high resolution FT-ICR ESI-MS) = 502.6777 $[N_6]^{8+}$, 614.5039 $[N_6(NTf_2^-)]^{7+}$, 763.6273 $[N_6(NTf_2^-)_2]^{6+}$, 972.8152 $[N_6(NTf_2^-)_3]^{5+}$.

4 NMR spectra for NDI-edged Zn_4L_6 cage N_6

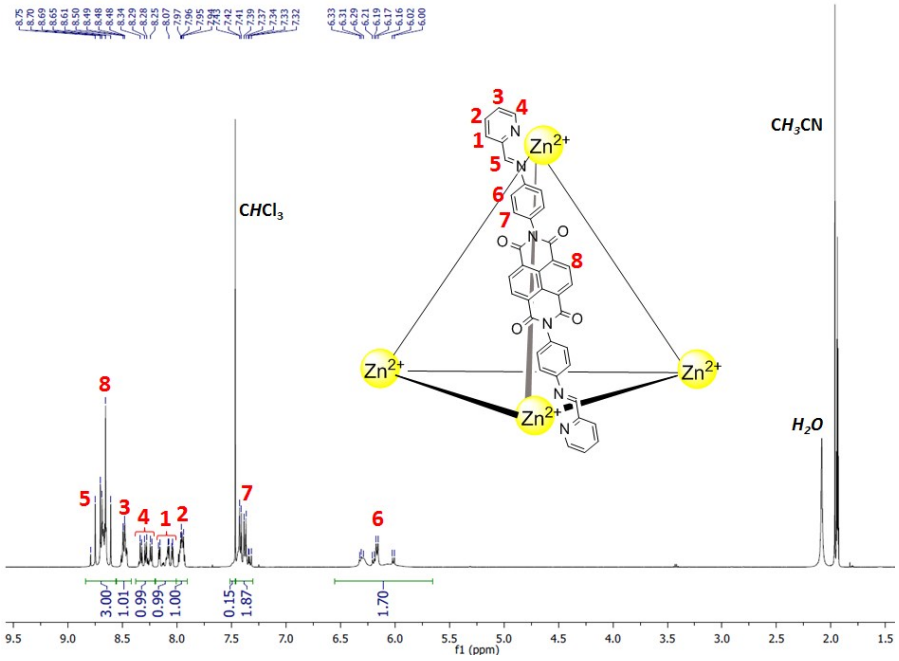

Figure S3. ^{1}H NMR (500 MHz: $CD_3CN/CHCl_3$ 1:1) of $\mathbf{N_6}$ with assignments. $\mathbf{N_6}$ exists predominantly the low symmetry S_4 diastereomer along with a smaller proportion of the T and C_3 diastereomers; several signals per ligand environment were therefore observed. Mixtures of diastereomers have been observed and reported in previous studies of M_4L_6 tetrahedral assemblies.[1]

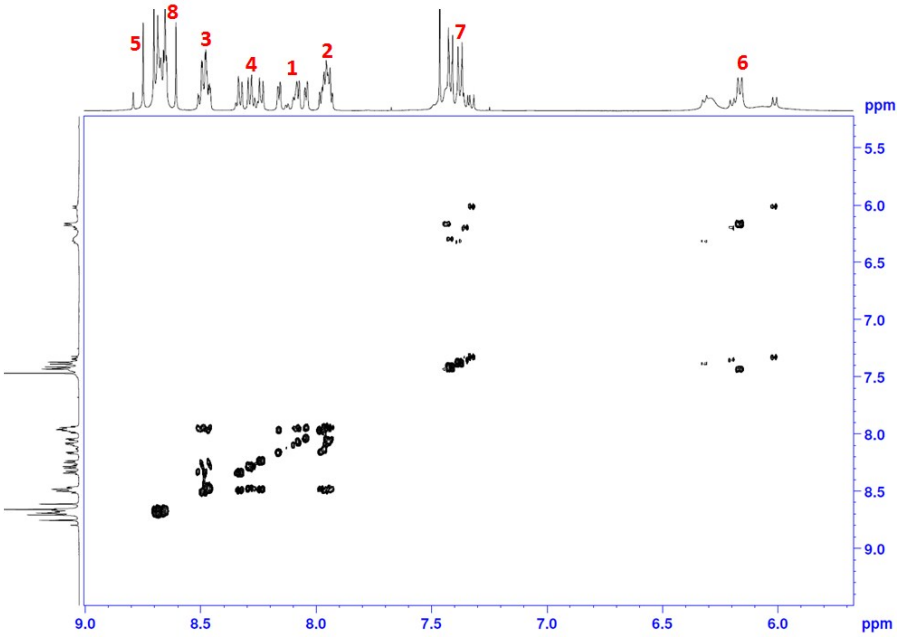

Figure S4. COSY NMR (500 MHz: $CD_3CN/CHCl_3$ 1:1, 298K) of $\mathbf{N_6}$.

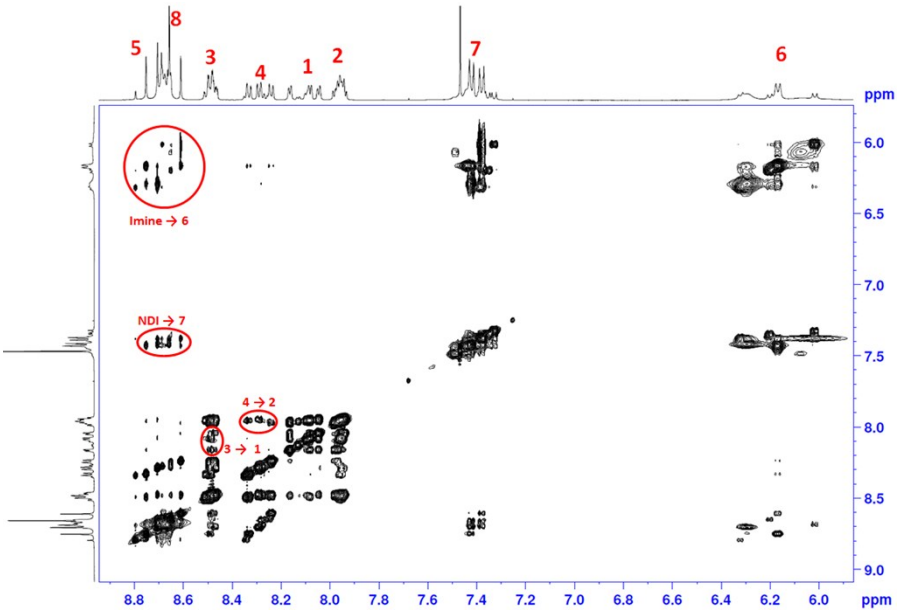

Figure S5. NOESY NMR (500 MHz: $CD_3CN/CHCl_3$ 1:1) of $\mathbf{N_6}$.

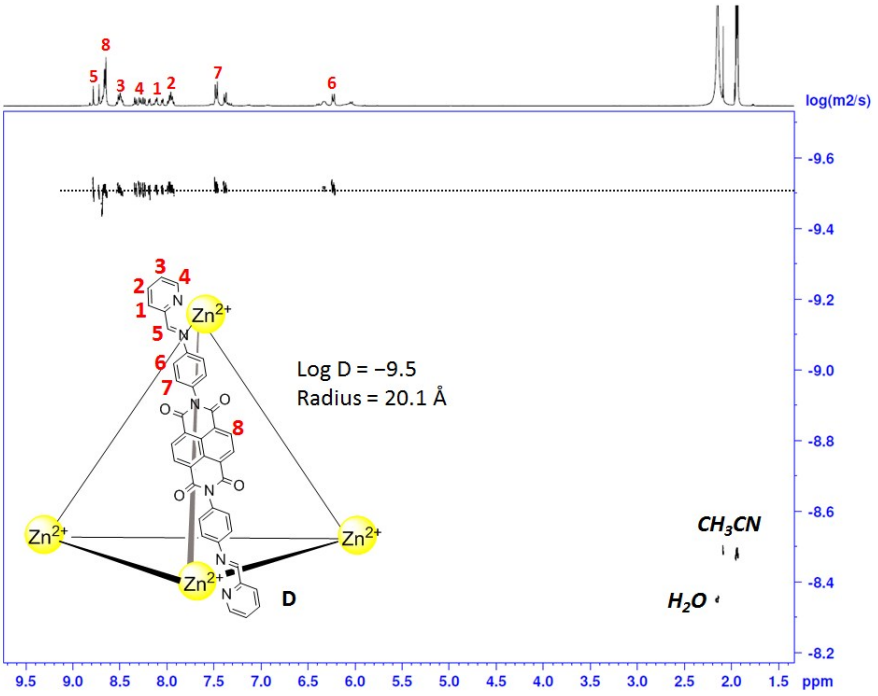

Figure S6. DOSY NMR spectrum (400 MHz: CD_3CN) of Zn_4L_6 $\mathbf{N_6}$ with assignments.

5 NMR Analysis of the interaction between N_6 and C

Solid $\mathbf{N_6}$ (6.26 mg, 1 μM) was added to a J-Young NMR tube and dissolved with 250 μL of 1:1 $CD_3CN/CDCl_3$. A solution of **C** (6.36 mg in 250 μL of 1:1 $CD_3CN/CDCl_3$, 10 μM) was added into the solution of $\mathbf{N_6}$, and the cap was sealed. This tube was briefly shaken to obtain a homogenous solution then left to equilibrate over 48h. ^{1}H NMR of the sample showed the occurrence of multiple new resonances similar to those observed in our previous system[2] and indicative of the formation of catenated adducts between $\mathbf{N_6}$ and **C**.

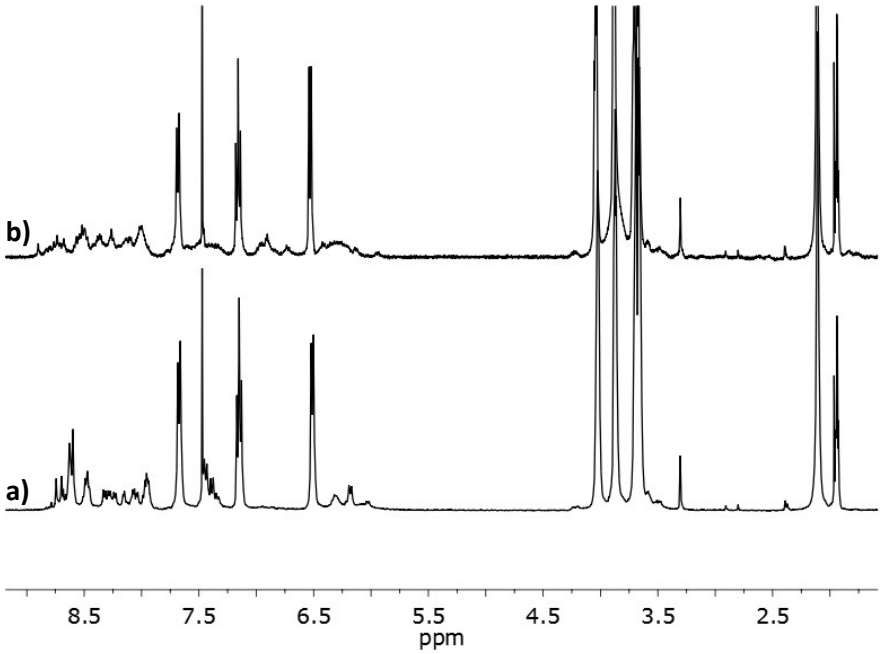

Figure S7. ^{1}H NMR spectra (400 MHz: CD_3CN/CD_3Cl 1:1) of $\mathbf{N_6}$ and **C** (10 equivalents) at a) time = 0 min and b) after 400 min (top).

6 Synthesis of porphyrin diamine 2

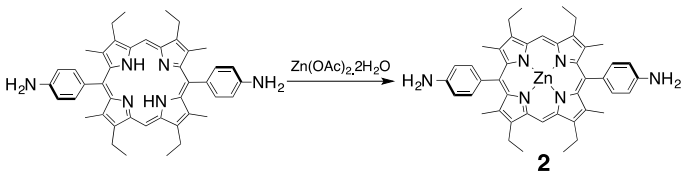

4,4'-(2,8,12,18-tetraethyl-3,7,13,17-tetramethylporphyrin-5,15-diyl)dianiline precursor was prepared by a previously reported method.[3]

4,4'-(2,8,12,18-tetraethyl-3,7,13,17-tetramethylporphyrin-5,15-diyl)dianiline (100 mg, 0.15 mmol) was dissolved in $CHCl_3$ (20 mL). A solution of zinc acetate dihydrate (132 mg, 0.60 mmol) in methanol (5 mL) was added and the solution was stirred at rt for 5 h. The solution was washed with H_2O (2 x 50 mL), the organic solution was retained and dried with $MgSO_4$. The solution was concentrated *in vacuo* then precipitated from hexane to give a pink solid that was isolated by filtration and dried (91 mg, 0.13 mmol, 87 %); ^{1}H NMR (400 MHz, $CDCl_3$) δ = 10.16 (2H, s), 7.78 (4H, d, *J* = 8.36 Hz) 7.01 (4H, d, *J* = 8.36 Hz) 4.01 (8H, q, *J* = 7.95 Hz), 3.91 (4H, s), 2.58 (12H, s), 1.77 (12H, t, *J* = 7.95 Hz); ^{13}C NMR (125 MHz, $CDCl_3$) δ = 148.6, 146.2, 146.1, 144.6, 138.2, 134.5, 134.0, 119.6, 114.5, 97.0, 20.1, 17.8, 15.5; *m/z* (ESI-MS) = 723.3 [**2**]$^+$; Elemental analysis calcd (%) for $C_{44}H_{46}N_6Zn{\cdot}0.4CHCl_3$ = C 69.08, H 6.06, N 10.89, found: C 69.00, H 5.96, N 10.52; m.p. = decomposition observed at >300 ˚C.

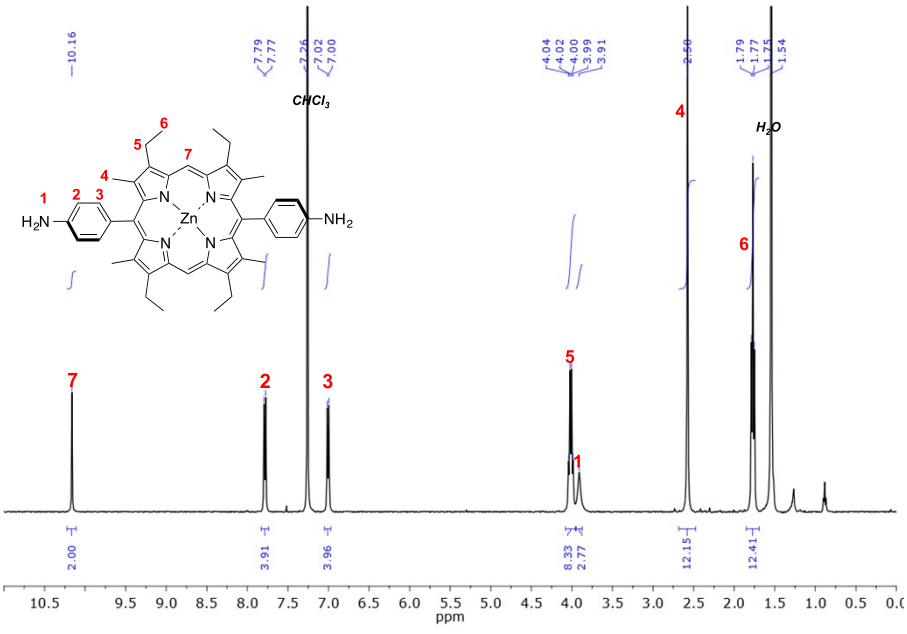

Figure S8: ^{1}H NMR (400 MHz, $CDCl_3$) spectrum of **2** with assignments.

7 Synthesis of porphyrin Zn_4L_6 cage P_6.

Porphyrin **2** (40.0 mg, 55 μmol), zinc(II) triflimide (23.0 mg, 37 μmol) and 2-formylpyridine (10.5 μL, 110 μmol) were combined in MeCN/$CHCl_3$ (7:3, 20 mL) and sonicated. The resultant red solution was heated at 343 K under N_2 for 16 h. The solution was concentrated *in vacuo* then added dropwise into diethyl ether. The resultant precipitate was isolated by filtration through Celite, washed with additional Et_2O, and then redissolved in MeCN. The solution was reduced to dryness to give a dark red powder (65.0 mg, 89%); ^{1}H NMR (500 MHz, CD_3CN) δ 10.06 – 9.62 (m, 1H), 9.28 (m, 1H), 8.73 – 8.25 (m, 3H), 8.20 – 7.87 (m, 3H), 7.63 – 7.27 (m, 3H), 4.11 – 3.36 (m, 4H), 2.52 – 2.06 (m, 6H), 1.77 – 0.83 (m, 6H); ^{13}C NMR (125 MHz, CD_3CN) δ = 166.2, 165.5, 165.0, 151.0, 150.7, 150.4, 148.5, 148.1, 148.0, 147.9, 147.8, 147.7, 146.8, 146.7, 146.6, 146.5, 146.4, 146.2, 146.0, 145.9, 145.8, 145.8, 144.0, 138.0, 137.8, 135.5, 132.1, 131.9, 131.8, 131.5, 124.8, 122.5, 122.3, 122.2, 122.1, 98.0, 97.9, 97.7, 20.4, 20.3, 20.2, 20.0, 18.1, 17.9, 17.9, 17.6, 16.4, 16.3, 16.2, 16.2; *m/z* (high resolution FT-ICR ESI-MS) = 709.6964 $[\mathbf{P_6}]^{8+}$, 851.1489 $[\mathbf{P_6}(NTf_2)]^{7+}$, 1040.1088 $[\mathbf{P_6}(NTf_2)_2]^{6+}$; Elemental analysis calcd (%) for $C_{352}H_{312}F_{48}N_{56}O_{32}S_{16}Zn_{10}\cdot 3H_2O\cdot 4CHCl_3$ = C 50.61, H 3.84, N 9.28, found: C 50.88, H 3.68, N 9.00.

8 Spectra for porphyrin-edged Zn_4L_6 cage P_6

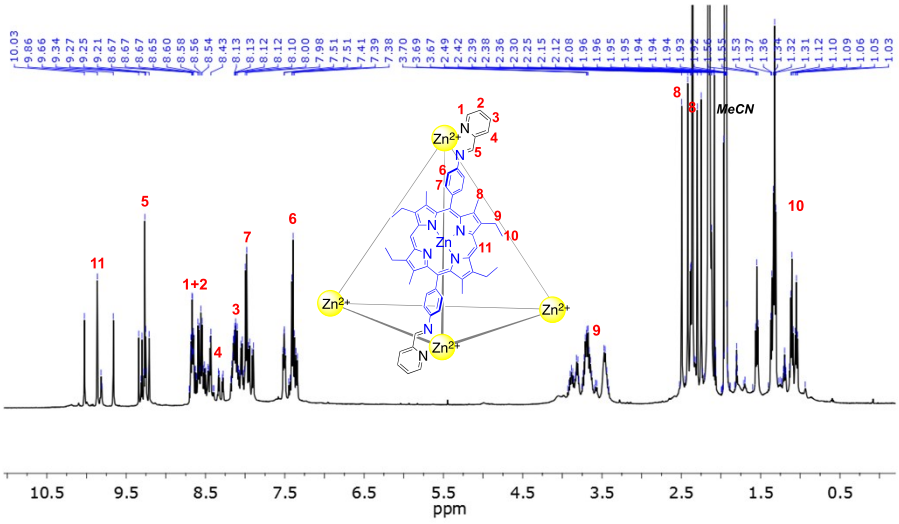

Figure S9. ^{1}H NMR spectrum (500 MHz, CD_3CN) of $\mathbf{P_6}$.

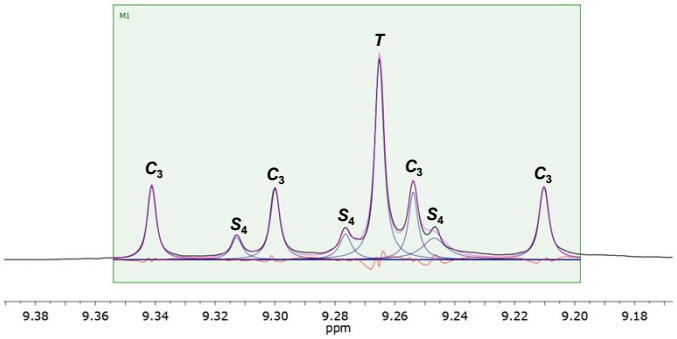

Figure S10. Imine-H resonances in the ^{1}H NMR (500 MHz, CD_3CN) spectrum of $\mathbf{P_6}$. Labels indicate which of 3 diastereomeric forms of $\mathbf{P_6}$ each resonance corresponds to.[1]

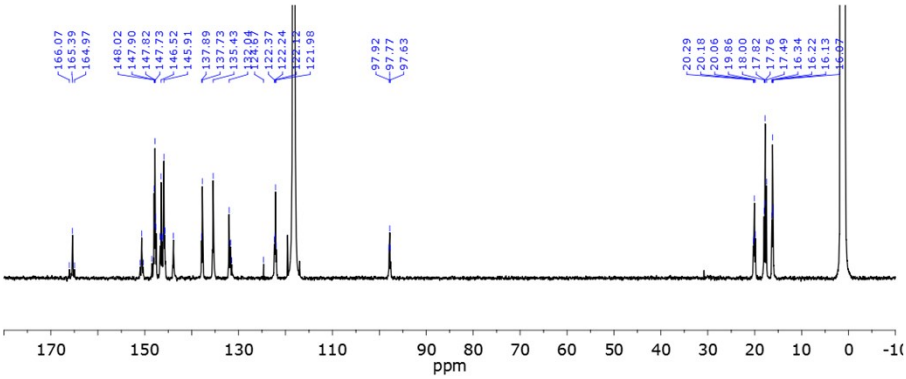

Figure S11. ^{13}C NMR (125 MHz, CD_3CN) spectrum of $\mathbf{P_6}$.

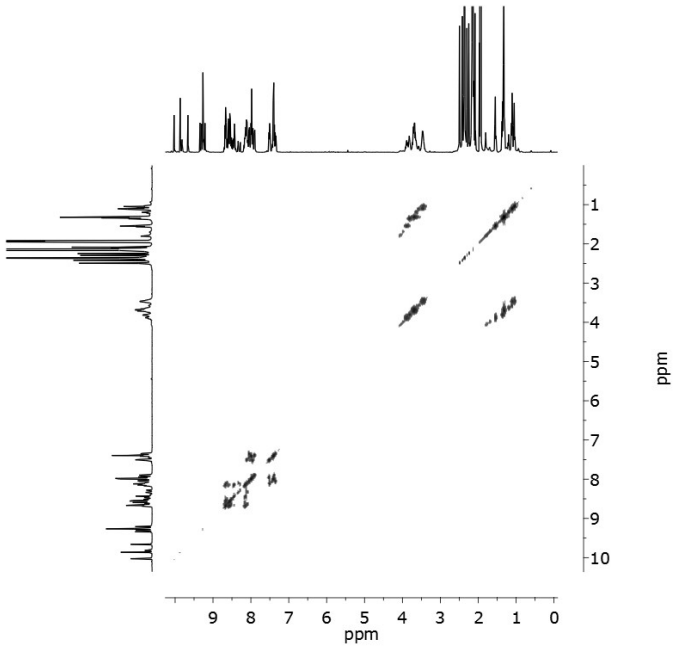

Figure S12. ^{1}H-^{1}H COSY NMR (500 MHz, CD_3CN) spectrum of $\mathbf{P_6}$.

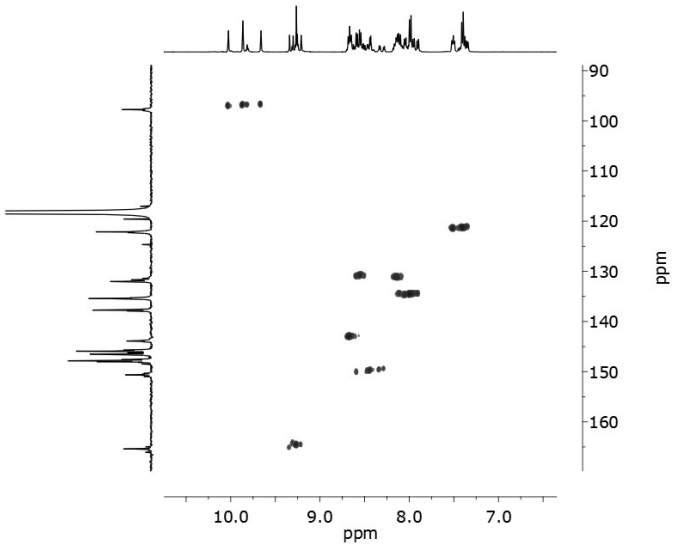

Figure S13. Aromatic region of the HSQC spectrum (CD_3CN) of $\mathbf{P_6}$.

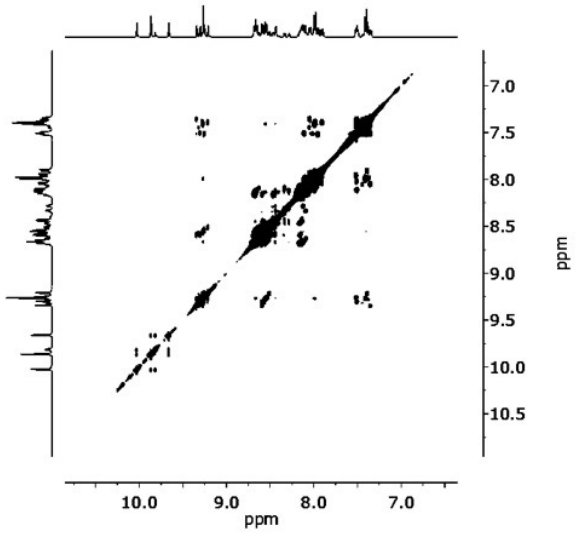

Figure S14. Aromatic region of the NOESY NMR spectrum (CD_3CN) of $\mathbf{P_6}$.

9 Preparation of host-guest complex $C_{70}\subset P_6$

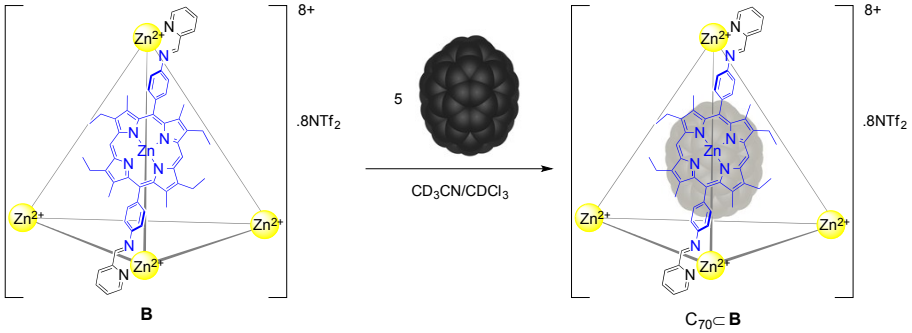

2 (4.0 mg, 5.5 µmol), $Zn(NTf)_2$ (2.3 mg, 3.7 µmol) and 2-formylpyridine (1.1 µL, 11 µmol) were combined in $CD_3CN/CDCl_3$ (7:3, 0.7 mL) and sonicated. The resultant red solution was heated at 323 K for 16 h. C_{70} (4.0 mg, 4.7 µmol) was added to the solution followed by sonication and heating at 323 K for a further 24h. On completion, the solution was added dropwise into Et_2O. The resultant precipitate was isolated by filtration through Celite, washed with additional Et_2O, then redissolved in MeCN. The solution was reduced to dryness to give a dark red powder (6.9 mg, 0.8 µmol, 87 %); ^{1}H NMR (500 MHz, CD_3CN) δ 9.94 – 9.62 (m, 1H), 9.39 – 9.09 (m, 1H), 8.76 – 8.61 (m, 1H), 8.61 – 8.50 (m, 1H), 8.47 – 8.28 (m, 1H), 8.16 – 8.07 (m, 1H), 7.99 (br, 2H), 7.63 – 7.25 (m, 2H), 4.24 – 3.31 (m, 4H), 2.59 – 2.21 (m, 6H), 1.60 – 0.81 (m, 6H); ^{13}C NMR (125 MHz, CD_3CN) δ = 165.96, 165.46, 150.72, 148.32, 148.05, 147.95, 147.83, 146.98, 146.79, 146.73, 146.65, 146.35, 146.21, 146.07, 145.92, 143.90, 143.83, 143.49, 143.12, 141.07, 140.68, 137.26, 135.51, 132.16, 131.83, 126.56, 126.00, 124.77, 122.42, 122.22, 98.24, 20.11, 17.94, 17.88, 17.69, 16.24, 15.62; *m/z* (high resolution FTICR ESI-MS) = 814.8504 $[C_{70}\subset\mathbf{P_6}]^{8+}$, 971.3282 $[C_{70}\subset\mathbf{P_6}(NTf_2)]^{7+}$; Elemental analysis calcd (%) for $C_{422}H_{312}F_{48}N_{56}O_{32}S_{16}Zn_{10}\cdot 12CHCl_3$ = C 54.29, H 3.40, N 8.17, found: C 54.41, H 3.51, N 7.84.

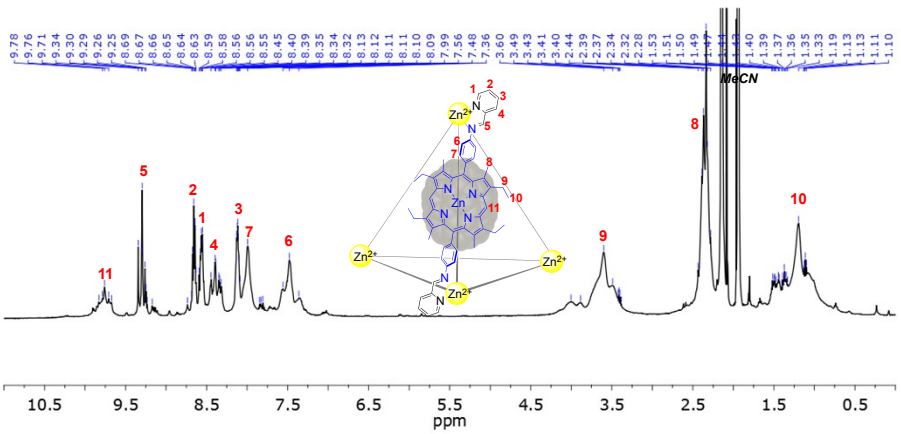

Figure S15. ^{1}H NMR (500 MHz, CD_3CN) spectrum of $C_{70}\subset\mathbf{P_6}$

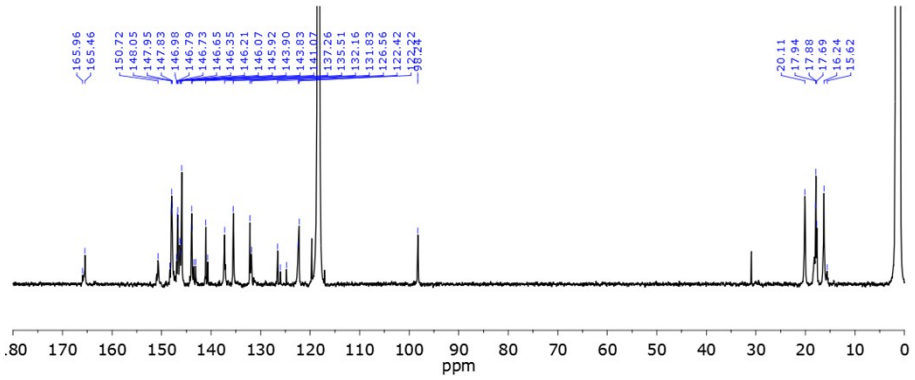

Figure S16. ^{13}C NMR (125 MHz, CD_3CN) spectrum of $C_{70}\subset$**P**$_6$, showing new resonances between 140-145 ppm corresponding to C_{70}.

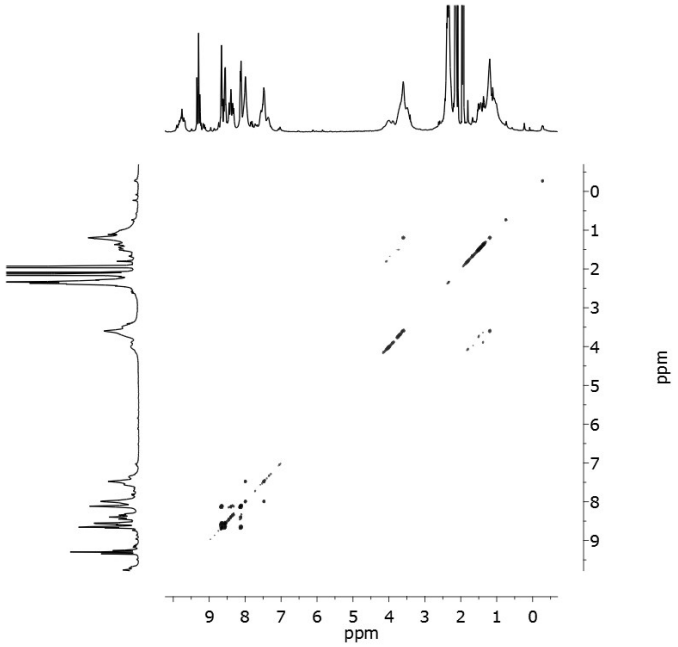

Figure S17. ^{1}H-^{1}H COSY (500 MHz, CD_3CN) spectrum of $C_{70}\subset$**P**$_6$.

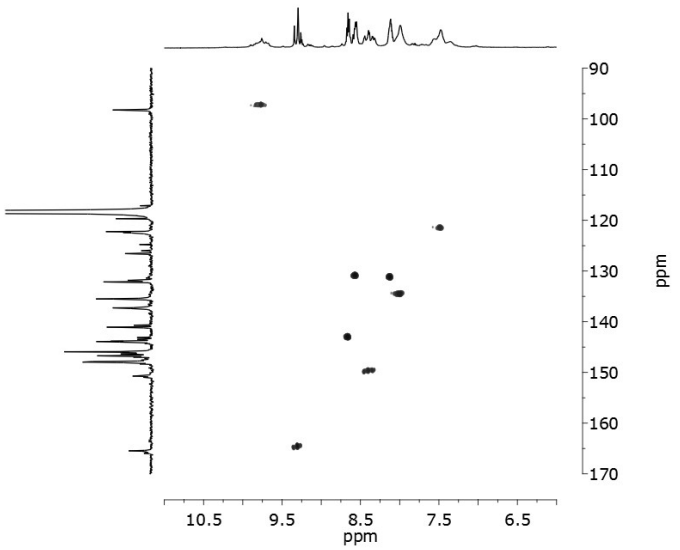

Figure S18. Aromatic region of the HSQC spectrum (CD_3CN) of $C_{70}\subset\mathbf{P_6}$.

10 Interactions between P_6 and C

It was anticipated that the porphyrin components of $\mathbf{P_6}$ would be too bulky to allow catenation to occur with **C**. To investigate this, an experiment was conducted where $\mathbf{P_6}$ and **C** were mixed in a 1:1 ratio in a 1:1 solution of $CDCl_3$ and CD_3CN. The solution was analysed by ^{1}H NMR immediately after mixing (Figure S19) and no further change in the spectrum was observed after heating to 323 K for 2 h. The resultant NMR spectrum showed the presence of broad resonances between 6-7 ppm that correspond to the aromatic protons of **C**. The upfield shift of these resonances is indicative of an interaction between the naphthalene units in **C** and $\mathbf{P_6}$, however, their rapid appearance and broadness are consistent with a fast-exchange process whereby π-interactions occur without a catenation event taking place. As observed in the case of $\mathbf{N_6}$ and in our previously reported system,[2] the formation of catenanes with **C** yields sharp NMR resonances consistent with a specific interaction between **C** and the tetrahedral assemblies.

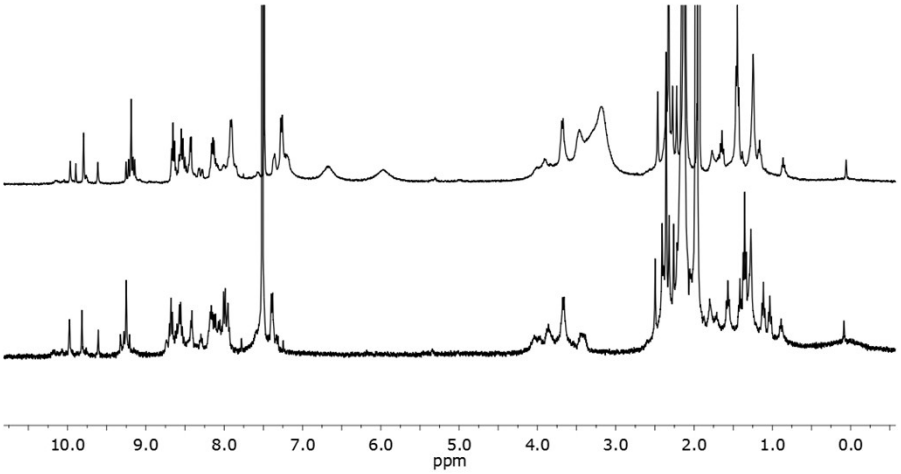

Figure S19. ^{1}H NMR (400 MHz, 1:1 $CD_3CN/CDCl_3$) spectrum of $\mathbf{P_6}$ (bottom) and $\mathbf{P_6}$ and **C** (1 equiv, top).

11 Infrared multiphoton dissociation (IRMPD) MS/MS of catenated cages

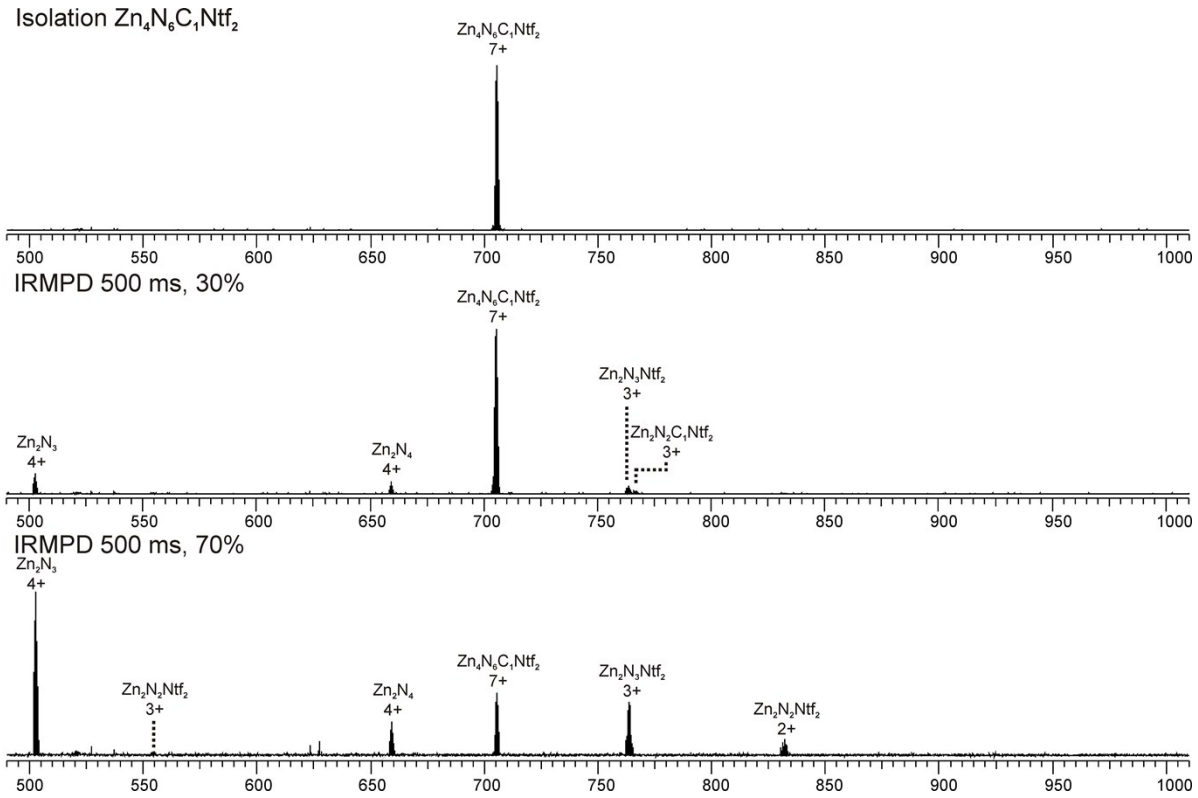

Figure S20: ESI-FTICR MS isolation and fragmentation of $[Zn_4N_6C_1(NTf_2)]^{7+}$ (*m/z* = 704).

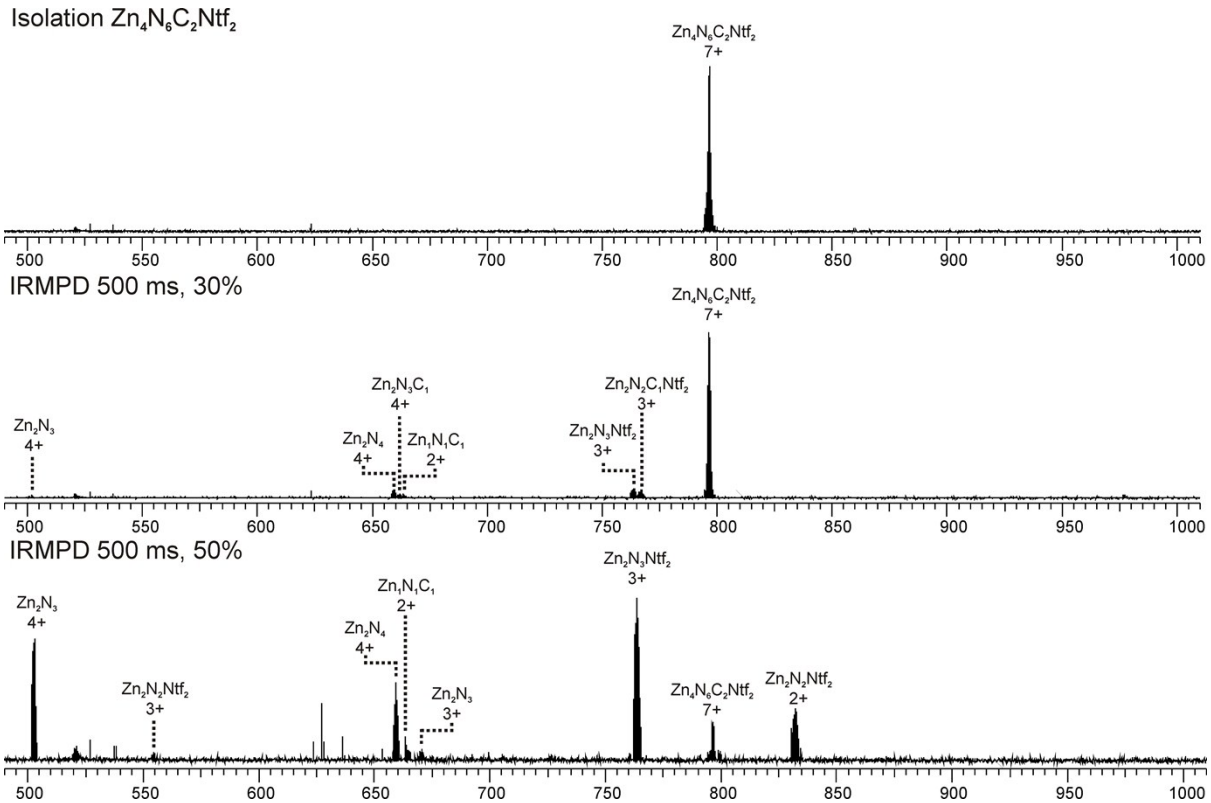

Figure S21: ESI-FTICR MS isolation and fragmentation of $[Zn_4N_6C_2(NTf_2)]^{7+}$ (*m/z* = 795).

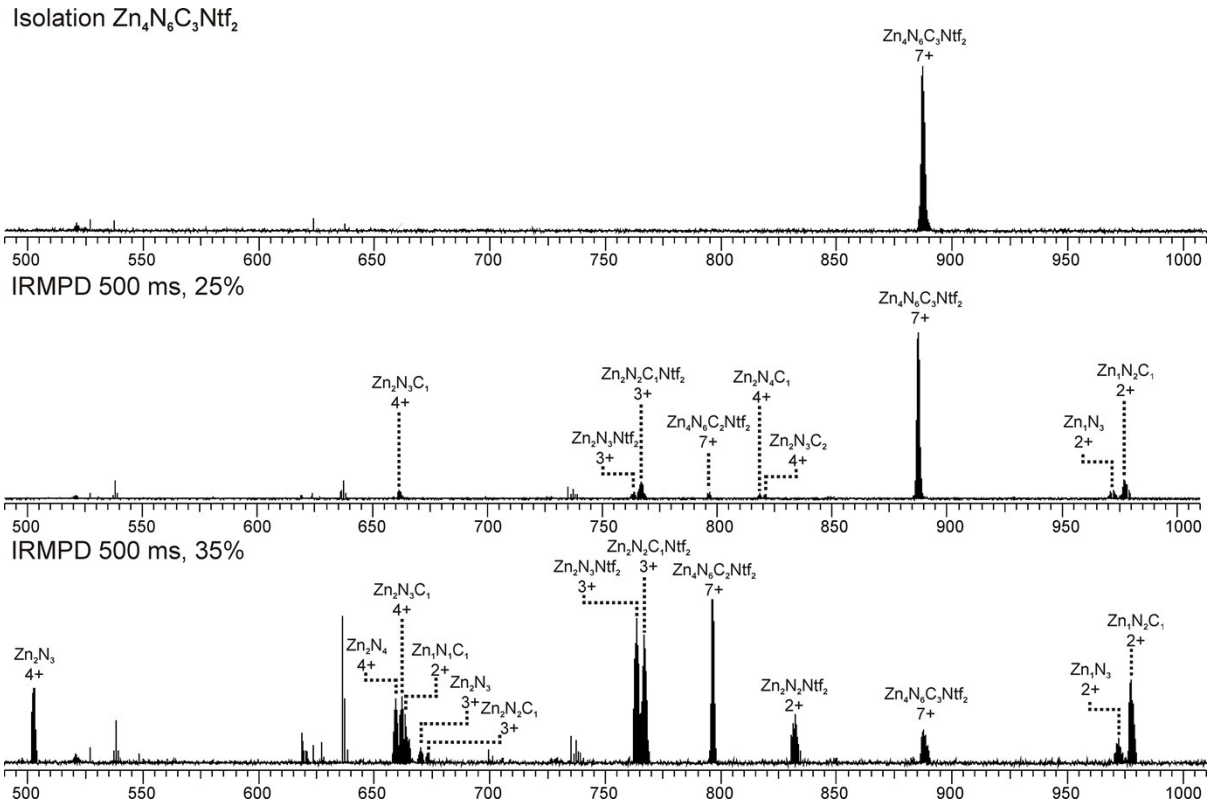

Figure S22: ESI-FTICR MS isolation and fragmentation of $[Zn_4N_6C_3(NTf_2)]^{7+}$ (*m/z* = 887).

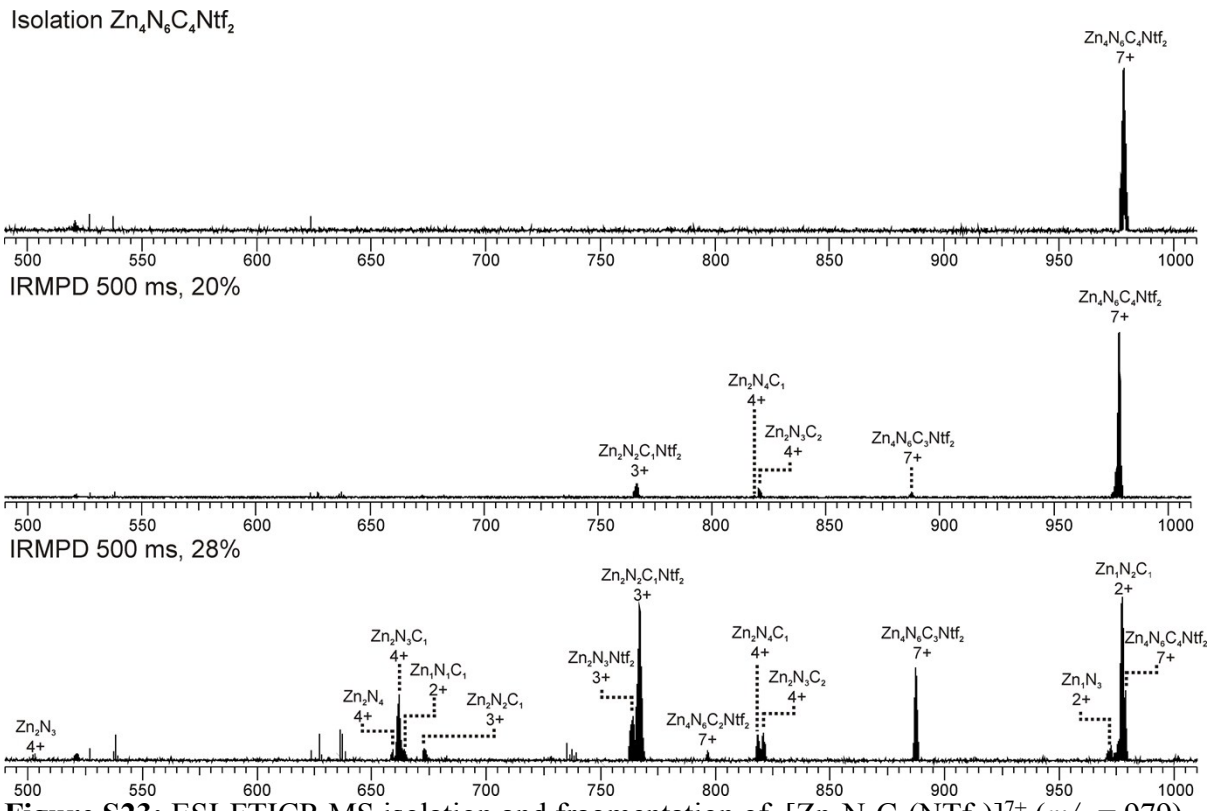

Figure S23: ESI-FTICR MS isolation and fragmentation of $[Zn_4N_6C_4(NTf_2)]^{7+}$ (*m/z* = 979).

12 Analysis of a mixed ligand cage DCL

General procedure for DCL Preparation.

For ESI-MS analysis DCLs were created using 1:1 mixtures of the purified cages $\mathbf{N_6}$ and $\mathbf{P_6}$ (1:1 MeCN/$CHCl_3$, 1mM). These solutions were combined in glass vials and allowed to equilibrate at room temperature for at least 24 h. For ESI-MS measurements the solutions were extracted, diluted (25 μM) and mixed by hand for 1 min before injection.

For templation studies, C_{70} was added as a solid (4 equivalents relative to total cage content) to an equilibrated DCL solution. **C** was synthesized using the methods previously described[2] and was also introduced to equilibrated DCL as a solid (0.5 or 4 equivalents). Templated libraries were allowed to re-equilibrate at room temperature for a further 24 h prior to ESI-MS analysis.

Procedure for DCL Analysis.

MS data were processed using the instrument's Omega MS software.[5] In each experiment, the intensities of the + 8 and + 7 charge states of each species were summed to give an overall observable intensity per species. These values were combined for all species with the same **N**:**P** ratio (*i.e.* including host-guest adducts). Once summed, all intensities were normalized with respect to the maximum signal intensity obtained. These values were then plotted to give the relative distribution of the $\mathbf{N_xP_{(6-x)}}$ species (Figure 6 in the main text).

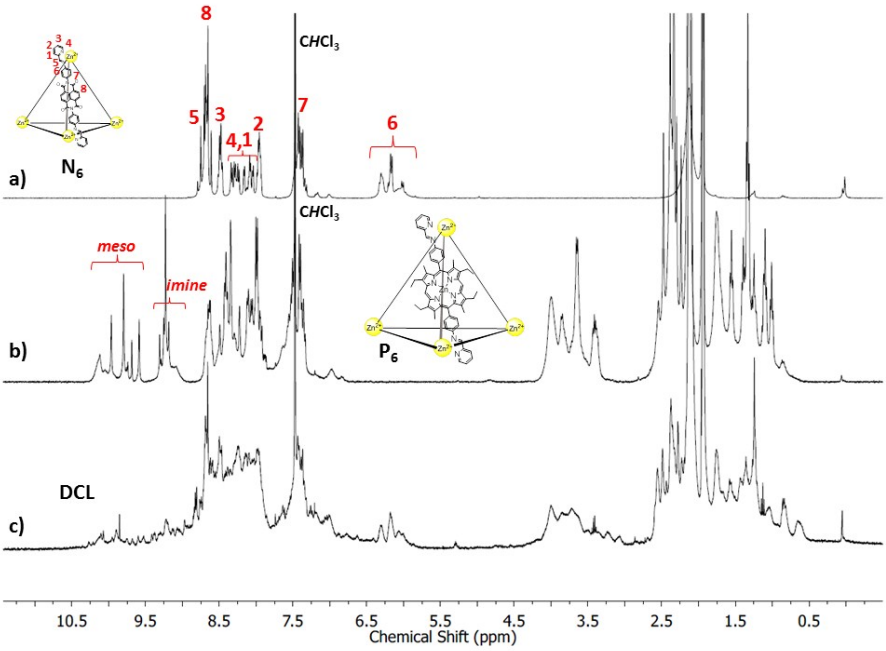

Figure S24: ^{1}H NMR (400 MHz, 1:1 $CD_3CN/CDCl_3$) spectra of a) $\mathbf{N_6}$, b) $\mathbf{P_6}$ and c) the DCL obtained from a 1:1 mixture of $\mathbf{N_6}$ and $\mathbf{P_6}$ 24h after mixing.

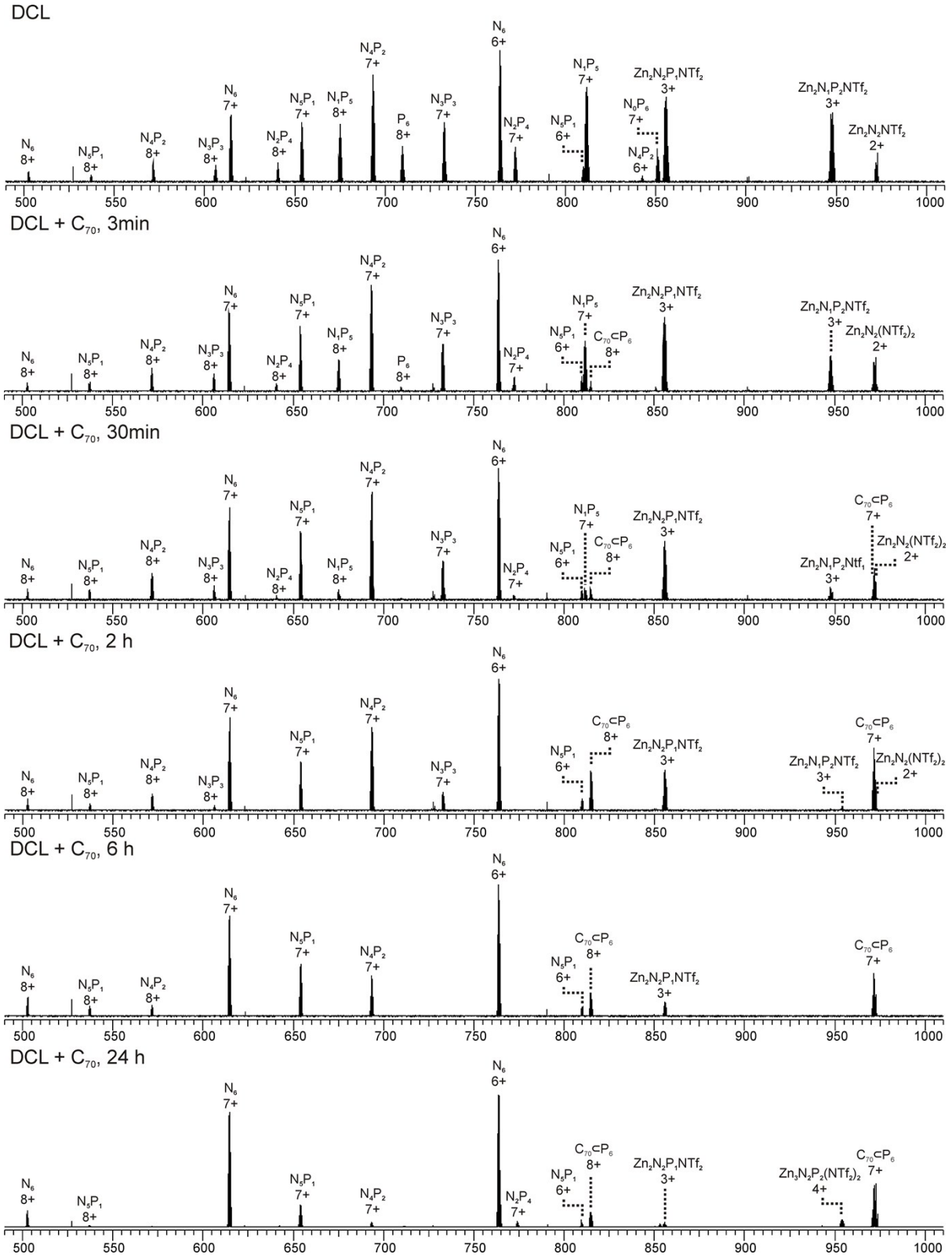

Figure S25: ESI-FTICR-MS spectra of DCL + C_{70} (4 equiv.) at different time intervals.

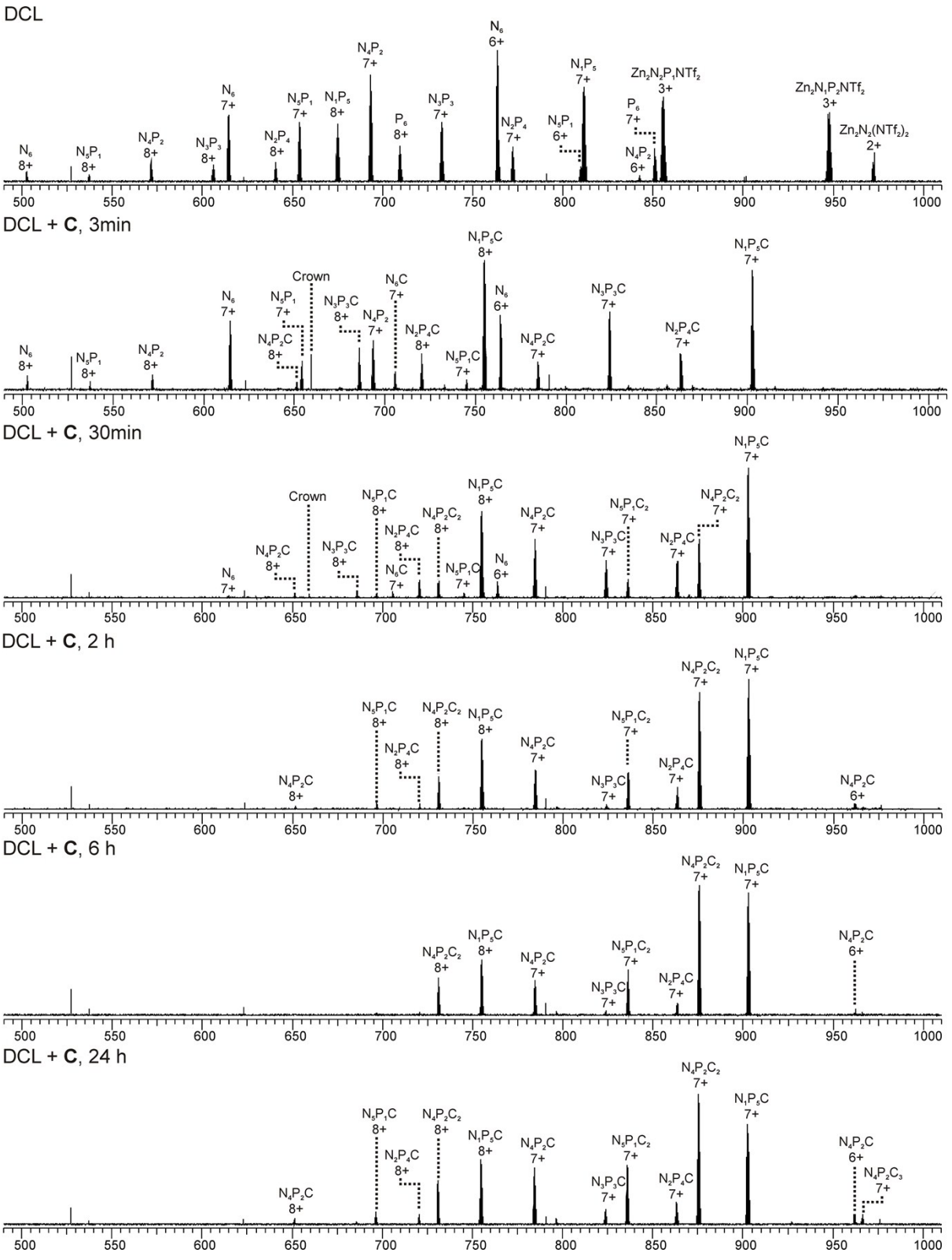

Figure S26: ESI-FTICR-MS spectra of DCL + **C** (4 equiv.) taken at different time intervals.

As a control experiment to confirm the equilibrium state, a DCL was prepared by an independent synthesis from a mixture of all building blocks and not as usual from the purified cages.

Therefore, porphyrin ligand (7.24 mg, 0.01 mM), NDI ligand (4.48 mg, 0.01 mM) and metal salt (0.0133 mM, 9.39 mg for $Fe[NTf_2]_2 \cdot 5H_2O$ or 8.32 mg for $Zn[NTf_2]_2$ were added to a flask. 2ml of MeCN and 2ml of $CHCl_3$ were added and the reaction mixed was sonicated in a warm ultrasonicator bath for 30 mins. 2-pyridinecarboxylate (0.02 mM, 2.14 mg) was then added to the suspension and the reaction was allowed to equilibrate for 7d at 50°C.

A sample of the mixture was filtered, diluted to 25µM and subjected to MS analysis.

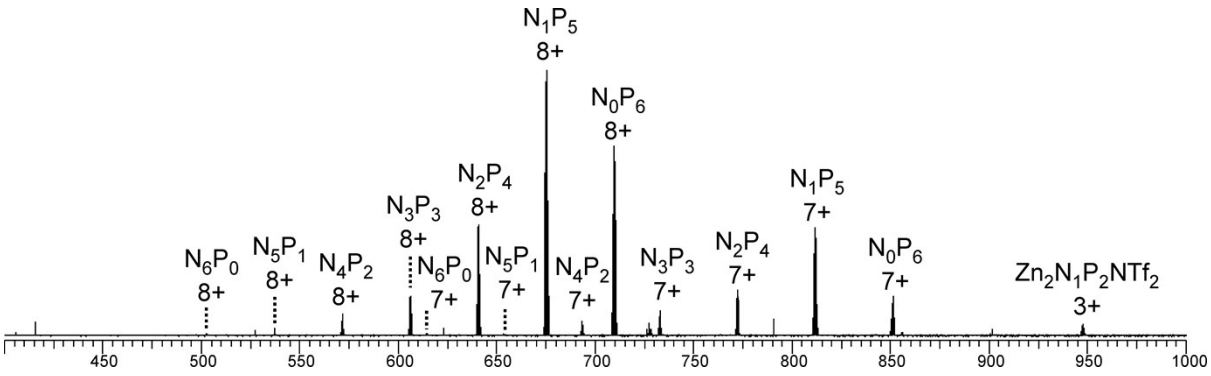

Figure S27: ESI-FTICR-MS spectrum of a DCL formed from ligands.

The distribution of mixed cages in this experiment is not in agreement with distribution in the DCL synthesized from pre formed cages. Due to the very poor solubility of the NDI ligand, a strong excess of porphyrin-ligand is present in solution, leading to an excess of porphyrin-rich cages in the DCL.

To investigate whether $\mathbf{N_1P_5}$ could be formed exclusively, the general procedure for DCL preparation was followed using 1:5 mixture of $\mathbf{N_6}$ and $\mathbf{P_6}$. Subsequent MS analysis showed that a $\mathbf{N_xP_{(6-x)}}$ was still formed rather than a single produce. The distribution of mixed cages is noticeably different to the 1:1 mixtures of $\mathbf{N_6}$ and $\mathbf{P_6}$, which is unsurprising given the different proportion of library components.

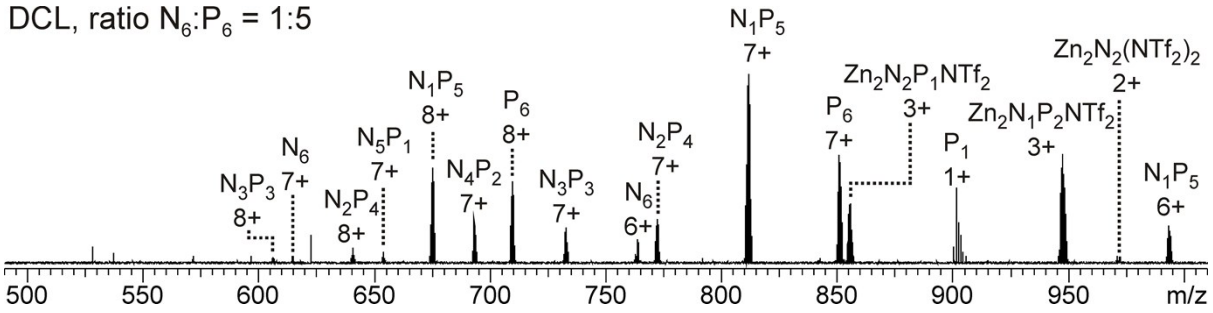

Figure S28: ESI-FTICR-MS spectrum of a DCL formed from a 1:5 mixture of **N_6** and **P_6**.

13 X-ray Crystallography

Data were collected with an Oxford Gemini Ultra employing confocal mirror monochromated Cu-Kα radiation generated from a sealed tube (1.5418 Å) with ω and ψ scans at 120(2) K[6] or at Beamline I19 of Diamond Light Source[7] employing silicon double crystal monochromated synchrotron radiation (0.6889 Å) with ω scans at 100(2) K.[8] Data integration and reduction were undertaken with CrysAlisPro[6] or with SAINT and XPREP[9] (following treatment with ECLIPSE[10]). Subsequent computations were carried out using the WinGX-32 or ShelXle[11] graphical user interface.[12] Gaussian absorption corrections were applied using CryAlisPro[6] and multi-scan empirical absorption corrections were applied to the data using SADABS.[9] Structures were solved by direct methods using SHELXT[13] or SUPERFLIP[14] then refined and extended with SHELXL.[13b] In general, non-hydrogen atoms with occupancies greater than 0.5 were refined anisotropically. Carbon-bound hydrogen atoms were included in idealized positions and refined using a riding model. Nitrogen and oxygen-bound hydrogen atoms were first located in the difference Fourier map before refinement. Disorder was modelled using standard crystallographic methods including constraints, restraints and rigid bodies where necessary. Crystallographic data along with specific details pertaining to the refinement follow. Crystallographic data have been deposited with the CCDC (CCDC 1061975 - 1061977).

2(MeOH)·0.5MeOH.

Formula $C_{45.5}H_{52.5}N_6O_{1.5}Zn$, M 772.80, Monoclinic, space group $P2_1$ (#4), a 8.3889(4), b 21.3112(10), c 11.1950(6) Å, β 93.127(3), V 1998.43(17) Å^3, D_c 1.284 g cm^{-3}, Z 2, crystal size 0.08 by 0.01 by 0.002 mm, colour red, habit needle, temperature 100(2) Kelvin, λ(synchrotron) 0.6889 Å, μ(synchrotron) 0.610 mm^{-1}, T(SADABS)$_{min,max}$ 0.6027, 0.7454, 2θmax 53.14, *hkl* range −10 10, −25 27, −14 14, N 26343, N_{ind}

8316(R_{merge} 0.0636), *N*obs 6057(I > 2σ(I)), N_{var} 525, residuals* *R*1(*F*) 0.0584, *wR*2(F^2) 0.1776, GoF(all) 1.045, $\Delta\rho_{min,max}$ −0.376, 1.262 e^- $Å^{-3}$.

Specific refinement details:

The zinc atom and coordinated methanol were modelled as disordered over two positions on opposite sides of the porphyrin ring with occupancies of 0.70 and 0.30. As a consequence of this disorder the structure displays strong pseudosymmetry. However structure solution in $P2_1/c$ (with the occupancies of the disordered parts fixed at 0.50 by symmetry) resulted in significantly worse residuals and the structure was thus refined as a racemic twin in $P2_1$ with the Flack parameter refining to 0.44(3).

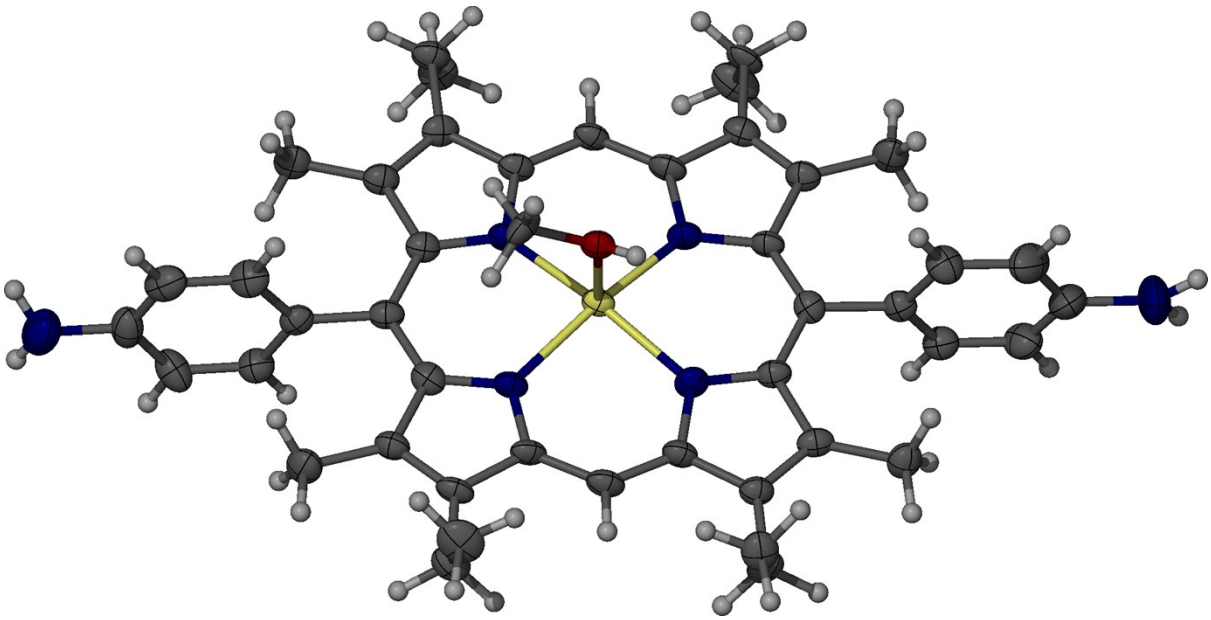

Figure S29: Crystal structure of **2**, with a single molecule of MeOH axially bound to the Zn center of the porphyrin (ORTEP 50%, disorder omitted for clarity). Zn = yellow, C = grey, H = white, N = blue, O = red.

Table S1. Hydrogen bonds in the structure of **2**(MeOH)·0.5MeOH [Å and °].

D-H...A	d(D-H)	d(H...A)	d(D...A)	<(DHA)
O(1)-H(1A)...N(5)#1	0.82	2.10	2.794(9)	142.5
N(5)-H(5A)...O(1A)#2	0.91	2.15	3.044(12)	167.8
N(6)-H(6B)...O(1A)#3	0.91	1.81	2.494(15)	130.4

Symmetry transformations used to generate equivalent atoms:
#1 -x,y+1/2,-z+1 #2 -x,y-1/2,-z #3 -x,y+1/2,-z

$[N_6]\cdot 5NTf_2\cdot 3PF_6$.

Formula $C_{230}H_{132}F_{24}N_{37}O_{28}P_3S_2Zn_4$, *M* 4736.23, Monoclinic, space group P 21/c (#14), *a* 29.307(5), *b* 45.110(9), *c* 26.896(6) Å, *b* 91.52(3), *V* 35545(12) Å3, D_c 0.885 g cm^{-3}, *Z* 4, crystal size 0.443 by 0.327 by 0.177 mm, colour yellow, habit block, temperature 120(2) Kelvin, λ(CuKa) 1.54184 Å, μ(CuKa) 1.310 mm^{-1}, $T(\text{CRYSALISPRO})_{min,max}$ 0.692, 1.287, $2\theta_{max}$ 77.62, *hkl* range −23 14, −36 36, −21 21, *N* 37642, N_{ind} 19847(R_{merge} 0.0526), *N*obs 15247(I > 2σ(I)), N_{var} 2953, residuals* *R*1(*F*) 0.1969, *wR*2(F^2) 0.5324, GoF(all) 2.255, $\Delta\rho_{min,max}$ -0.664, 0.923 e^- $Å^{-3}$.

Specific refinement details:

The crystals of $[\mathbf{N_6}]\cdot 5NTf_2\cdot 3PF_6$ were extremely unstable, immediately decaying once removed from the mother liquor and required rapid handling to facilitate data collection. This structure resembles that of a small protein in that only weak diffraction up to 1.2 Å resolution was achieved, resulting in poor quality data (e.g high R_{int} and wR_2). However the data are more than sufficient to establish the connectivity of the structure. Macromolecular refinement techniques were carefully adapted to build a molecular model, increase the robustness of the refinement and establish the connectivity of all modelled structural components with acceptable precision. To achieve this, similar organic building blocks in the structure (NDI ligands, PF_6^- and triflimide counter ions) were grouped into residues. Stereochemical restraint dictionaries[15] for each of these building blocks were generated with the GRADE program[16] using the GRADE Web Server[17] and applied in the structure refinement. The GRADE dictionary for SHELXL contains target values and standard deviations for 1,2-distances (DFIX) and 1,3-distances (DANG), as well as restraints for planar groups (FLAT). Local structural similarity[18] was exploited to make the geometries of NDI ligands similar using non-crystallographic symmetry restraints (NCSY) for 1,4 distances. The refinement of ADPs for all non-hydrogen atoms was enabled by employing similarity (SIMU) and enhanced rigid bond restraints (RIGU)[19] in SHELXL.[13b] Disordered solvent/counterion areas occupy 11% of the unit cell. In contrast to indications from refinement statistics, the final model is in good agreement with experimentally observed electron density (Figure S28).

Five anions per cage were significantly disordered; no satisfactory model for the electron-density associated with them could be found despite numerous attempts at modeling. Therefore the SQUEEZE[20] function of PLATON[21] was employed to remove the contribution of the electron density associated with these anions and further disordered solvent molecules.

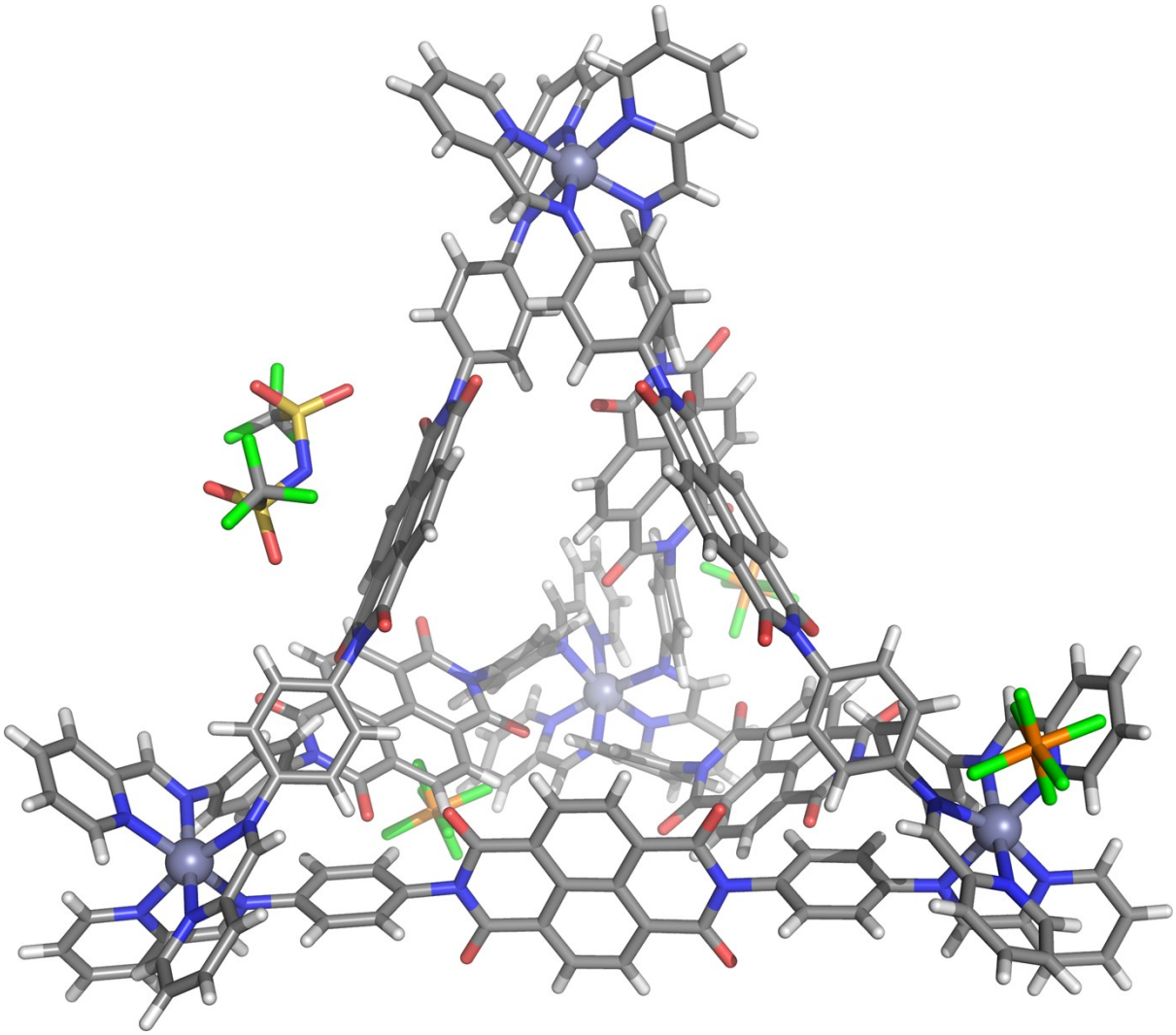

Figure S30. Atomic representation of the asymmetric unit of NDI cage $\mathbf{N_6}$ including all modelled hexafluorophosphate and triflimide counter ions.

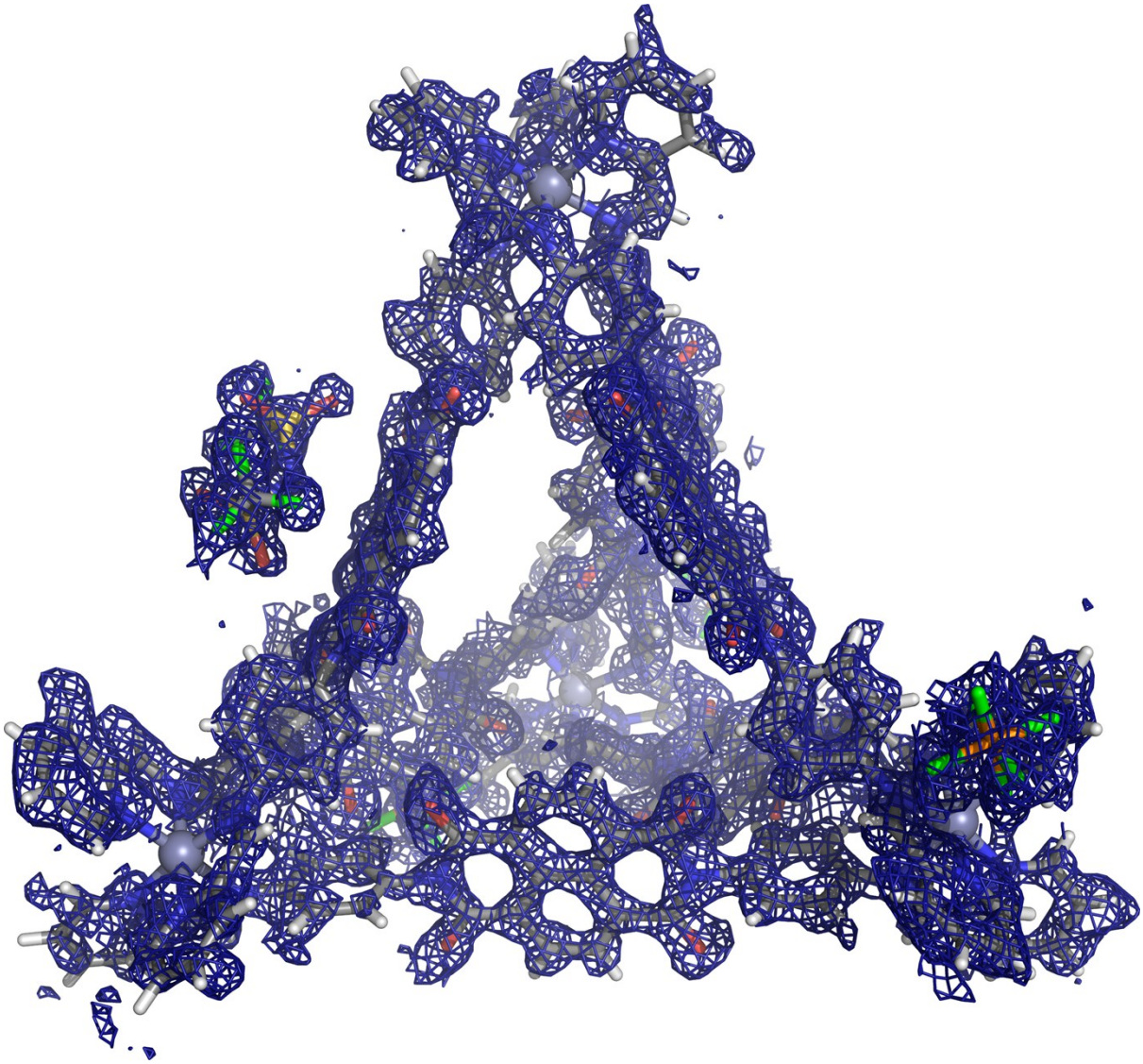

Figure S31. Atomic representation of the asymmetric unit of NDI cage $\mathbf{N_6}$ including all modelled hexafluorophosphate and triflimide counter ions. In addition to the previous figure the observed electron density (F_O) is shown as a blue mesh at 1.0 σ level, indicating a good fit of the final model into the observed electron density.

$[P_6(H_2O)_3(MeCN)_3]\cdot 8OTf$.

Formula $C_{350}H_{327}F_{24}N_{51}O_{27}S_8Zn_{10}$, M 7045.79, Trigonal, space group P-3c1 (#165), a 35.2240(14), b 35.2240(14), c 43.354(2) Å, γ120°, V 46584(4) Å^3, D_c 1.005 g cm^{-3}, Z 4, crystal size 0.010 by 0.010 by 0.002 mm, color dark red, habit block, temperature 100(2) Kelvin, λ(synchrotron) 0.6889 Å, μ(synchrotron) 0.522 mm^{-1}, $T(SADABS)_{min,max}$ 0.4689, 0.7440, 2θmax 33.36, *hkl* range −29 29, −29 29, −36 34, *N* 244576, N_{ind} 9422(R_{merge} 0.1946), Nobs 6832(I > 2σ(I)), N_{var} 1257, residuals* R1(*F*) 0.1034, wR2(F^2) 0.2977, GoF(all) 1.129, $\Delta\rho_{min,max}$ −0.284, 0.520 e$^-$ Å^{-3}.

Specific refinement details:

The crystals of $[\mathbf{P_6}(H_2O)_3(MeCN)_3]\cdot 8OTf$ were extremely unstable, immediately decaying once removed from the mother liquor and required rapid handling to facilitate data collection. The crystals were also weakly diffracting with very few reflections recorded at higher than 1.2 Å resolution despite the use of synchrotron radiation; however the data are more than sufficient to establish the connectivity of the structure. The tetrahedron lies astride a centre of symmetry such that one third of it is crystallographically unique. Three of the ethyl groups were modelled as disordered over two positions. There is a significant amount of thermal motion in the extremities of the molecule and extensive thermal parameter (SIMU and DELU were applied to all non-hydrogen atoms except for Zn) and bond length restraints (DFIX) were required to facilitate realistic modeling of the organic parts of the structures. Four anions per cage were significantly disordered; no satisfactory model for the electron-density associated with them could be found despite numerous attempts at modeling. Therefore the SQUEEZE[20] function of PLATON[21] was employed to remove the contribution of the electron density associated with these anions and further disordered solvent molecules.

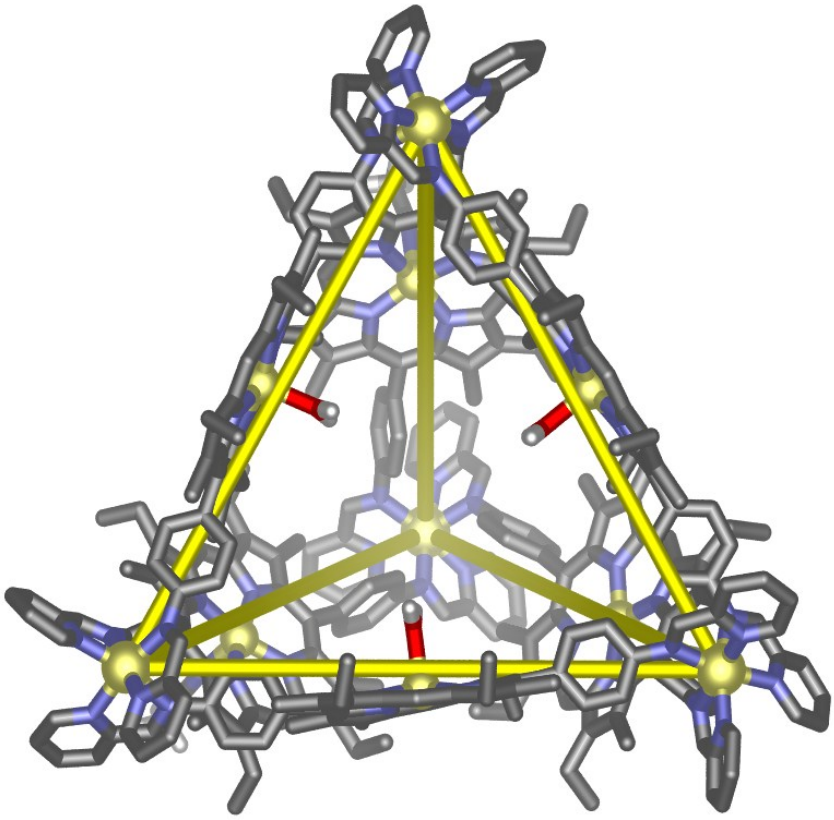

Figure S32: Representation of the crystal structure of $\mathbf{P_6}$, showing the three axial-bound water molecules directed inside the assembly. Yellow lines between the Zn^{II} atoms are included to highlight the tetrahedral framework. Hydrogen atoms (excluding those of H_2O), other solvent molecules, and anions are omitted for clarity. Zn = yellow, C = grey, H = white, N = blue, O = red.

14 References

1 a) W. Meng, J. K. Clegg, J. D. Thoburn and J. R. Nitschke, *J. Am. Chem. Soc.*, 2011, **133**, 13652-13660; b) T. Beissel, R. E. Powers, T. N. Parac and K. N. Raymond, *J. Am. Chem. Soc.*, 1999, **121**, 4200-4206.

2 S. P. Black, A. R. Stefankiewicz, M. M. J. Smulders, D. Sattler, C. A. Schalley, J. R. Nitschke and J. K. M. Sanders, *Angew. Chem. Int. Ed.*, 2013, **52**, 5749-5752.

3 D. M. Wood, W. Meng, T. K. Ronson, A. R. Stefankiewicz, J. K. M. Sanders and J. R. Nitschke, *Angew. Chem. Int. Ed.*, 2015, **54**, 3988-3992.

4 A. Vecchi, V. Grippo, B. Floris, A. G. Marrani, V. Conte and P. Galloni, *New. J. Chem.*, 2013, **37**, 3535-3542.

5 *Omega v9.2*, 2006, Varian Inc., Santa Clara, USA.

6 *CrysAlisPro*, 1.171.35.11 2009-2011, Agilent Technologies Yarton, Oxfordshire, UK.

7 H. Nowell, S. A. Barnett, K. E. Christensen, S. J. Teat and D. R. Allan, *J. Synchrotron Rad.*, 2012, **19**, 435.

8 *CrystalClear*, 2.0, 1997-2009, Rigaku Americas and Rigaku Corporation., 9009 TX, USA

9 Bruker-Nonius, *APEX, SAINT and XPREP*, 2013, Bruker AXS Inc., Madison, Wisconsin, USA.

10 *ECLIPSE*, 2004, ECLIPSE, University of Edinburgh, Edinburgh, UK.

11 C. B. Hubschle, G. M. Sheldrick and B. Dittrich, *J. Appl. Crystallogr.*, 2011, **44**, 1281-1284.

12 L. J. Farrugia, *J. Appl. Crystallogr.*, 1999, **32**, 837-838.

13 a) G. Sheldrick, *Acta Cryst.*, 2008, **A64**, 112-122; b) G. M. Sheldrick, *Acta. Cryst.*, 2015, **C71**, 3-8.

14 L. Palatinus and G. Chapuis, *J. Appl. Crystallogr.*, 2007, **40**, 786-790.

15 P. R. Evans, *Acta. Cryst.*, 2007, **D63**, 58-61.

16 *BUSTER*, 2.11.2, 2011, Global Phasing Ltd., Cambridge, United Kingdom.

17 *Grade Web Server*, 2014, Global Phasing Ltd. ,

18 O. S. Smart, T. O. Womack, C. Flensburg, P. Keller, W. Paciorek, A. Sharff, C. Vonrhein and G. Bricogne, *Acta. Cryst.*, 2012, **D68**, 368-380.

19 A. Thorn, B. Dittrich and G. M. Sheldrick, *Acta. Cryst.*, 2012, **A68**, 448-451.

20 a) P. van der Sluis and A. L. Spek, *Acta Cryst.*, 1990, **A46**, 194-201; b) A. L. Spek, *Acta. Cryst.*, 2015, **C71**, 9-18.

21 *PLATON: A Multipurpose Crystallographic Tool*, 2008, Utrecht University, Utrecht, The Netherlands.